JOURNAL OF BACTERIOLOGY, May 2007, p. 3525–3531 Vol. 189, No. 9
0021-9193/07/$08.00+0 doi:10.1128/JB.00044-07

Role of PBP1 in Cell Division of *Staphylococcus aureus*▽

S. F. F. Pereira,[1] A. O. Henriques,[2] M. G. Pinho,[3] H. de Lencastre,[1,4] and A. Tomasz[4]*

Laboratory of Molecular Genetics,[1] Laboratory of Microbial Development,[2] and Laboratory of Bacterial Cell Biology,[3] Instituto de Tecnologia Química e Biológica da Universidade Nova de Lisboa, 2780 Oeiras, Portugal, and Laboratory of Microbiology, The Rockefeller University, 1230 York Avenue, New York, New York 10021[4]

Received 9 January 2007/Accepted 8 February 2007

We constructed a conditional mutant of *pbpA* in which transcription of the gene was placed under the control of an IPTG (isopropyl-β-D-thiogalactopyranoside)-inducible promoter in order to explore the role of PBP1 in growth, cell wall structure, and cell division. A methicillin-resistant strain and an isogenic methicillin-susceptible strain, each carrying the *pbpA* mutation, were unable to grow in the absence of the inducer. Conditional mutants of *pbpA* transferred into IPTG-free medium underwent a four- to fivefold increase in cell mass, which was not accompanied by a proportional increase in viable titer. Examination of thin sections of such cells by transmission electron microscopy or fluorescence microscopy of intact cells with Nile red-stained membranes showed a morphologically heterogeneous population of bacteria with abnormally increased sizes, distorted axial ratios, and a deficit in the number of cells with completed septa. Immunofluorescence with an antibody specific for PBP1 localized the protein to sites of cell division. No alteration in the composition of peptidoglycan was detectable in *pbpA* conditional mutants grown in the presence of a suboptimal concentration of IPTG, which severely restricted the rate of growth, and the essential function of PBP1 could not be replaced by PBP2A present in methicillin-resistant cells. These observations suggest that PBP1 is not a major contributor to the cross-linking of peptidoglycan and that its essential function must be intimately integrated into the mechanism of cell division.

Penicillin-binding proteins (PBPs) are enzymes involved in the last stages of peptidoglycan biosynthesis. There are four native PBPs, PBP1 to PBP4, in *Staphylococcus aureus* and an additional PBP, PBP2A, in methicillin-resistant *S. aureus* (MRSA) strains (1, 5, 11). This extra PBP is encoded by the exogenous gene *mecA* and, in contrast to the native PBPs, shows low affinity for β-lactams, ensuring continued cell wall synthesis in the presence of otherwise lethal concentrations of these antibiotics (11, 25).

The primary amino acid structure of PBP1 shows a high degree of similarity to the sequences of PBP2B and SpoVD from *Bacillus subtilis*, PBP2X from *Streptococcus pneumoniae*, and PBP3 from *Escherichia coli* (33). All of these proteins are high-molecular-weight (HMW) class B PBPs, composed of a C-terminal domain with conserved transpeptidase motifs and an N-terminal domain of as-yet-unknown function (6, 7). Several lines of evidence indicate that PBP2B of *B. subtilis*, the pneumococcal PBP2X, and PBP3 of *E. coli* are involved in cell division (2, 20, 27, 34), consistent with their location in division and cell wall (*dcw*) synthesis clusters on the chromosome (28).

An earlier study by Pucci and colleagues has determined the chromosomal location of *S. aureus pbpA* in a *dcw* cluster together with other determinants, such as *mraY*, *divIB*, *ftsA*, and *ftsZ* (28), and a role for PBP1 in cell division of *S. aureus* has been proposed (22).

PBP1 of *S. aureus* was reported to be essential for growth because disruption of the chromosomal *pbpA* copy was lethal unless additional copies of the gene were present on a plasmid (33). However, the specific role(s) of PBP1 and its cellular address has not been investigated in detail.

The purpose of the studies described here was to construct a *pbpA* conditional mutant and use it to better define the essentiality of PBP1 for growth, to determine the contribution of PBP1 to the chemical structure of peptidoglycan, and to explore its role in cell division of *S. aureus*.

MATERIALS AND METHODS

Bacterial strains, media, and general methods. The strains and plasmids used in this study are listed in Table 1. The *mecA*-negative strain COL-S was constructed by introducing plasmid pSR (14), encoding the chromosomal cassette recombinase *ccrA* and *ccrB* genes, into strain COL and selecting for susceptibility to oxacillin, essentially as described previously (14), in order to excise the staphylococcal cassette chromosome *mec* (SCC*mec*) from the chromosome. *S. aureus* strains were grown at 37°C in tryptic soy broth (TSB) (Difco Laboratories, Detroit, MI) with vigorous aeration: 25-ml cultures were incubated in 250-ml Erlenmeyer flasks on a horizontal water bath shaker at a speed of 180 rpm. Alternatively, bacteria were plated on tryptic soy agar (Difco Laboratories). *E. coli* strains were grown at 37°C in Luria-Bertani (LB) broth (Difco Laboratories) with aeration or on LB agar (Difco Laboratories). Bacterial growth was monitored by measuring the optical density of *S. aureus* cultures at 620 nm (OD_{620}). Erythromycin and chloramphenicol were used at a concentration of 10 μg/ml for the selection of pMGP1- and pSK5632-derived *S. aureus* mutants, respectively. Conditional mutants were always grown in the presence of erythromycin and IPTG (isopropyl-β-D-thiogalactopyranoside) (Sigma, St. Louis, MO) at a concentration of 500 μM unless otherwise stated. DNA manipulations were performed according to standard procedures (17). The high-fidelity PfuTurbo DNA polymerase (Stratagene, Heidelberg, Germany) was used to generate PCR fragments for cloning; these were sequenced to ensure that no mutations had been introduced. *E. coli* strain DH5α was used for plasmid construction and propagation.

Construction of *pbpA* conditional mutants. An 850-bp fragment of *pbpA* was amplified from COL DNA by PCR using primers pbp1spacF (5′-GTACCCGGGACGATAATGTAAAGGTAG-3′ [SmaI site underlined]) and pbp1spacR (5′-TAGAGATCTGCATCCATGACAACCGC-3′ [BglII site underlined]). The amplified *pbpA* fragment and plasmid pMGPI (25) were digested with SmaI and BglII and ligated to create plasmid pMGPA. Plasmid pMGPA was introduced

* Corresponding author. Mailing address: The Rockefeller University, 1230 York Avenue, New York, NY 10021. Phone: (212) 327-8277. Fax: (212) 327-8688. E-mail: tomasz@mail.rockefeller.edu.

▽ Published ahead of print on 16 February 2007.

TABLE 1. Strains and plasmids

Strain or plasmid	Description[a]	Source or reference
S. aureus strains		
RN4220	Mc^s; restriction-negative derivative of 8325-4	R. Novick
COL	Homogeneous Mc^r Em^s Tc^s	The Rockefeller University Collection
COL-S	COL with SCC*mec* excised; Mc^s	This study
COL-S*spac*P1	COL-S with *pbpA* gene under P_{spac} control in the chromosome; Em^r	This study
COL*spac*P1	COL with *pbpA* gene under P_{spac} control in the chromosome; Em^r	This study
COLpSK5632	COL with pSK5632; Cm^r	This study
COL*spac*P1pSKP1	COL*spac*P1 with pSKP1; Em^r Cm^r	This study
LH607	8325-4; *spa* Tc^r	S. Foster
E. coli strain		
DH5α	*recA endA1 gyrA96 thi-1 hsdR17 supE44 relA1* ϕ80Δ*lacZ*Δ*M15*	Invitrogen
Plasmids		
pSR	Temperature-sensitive vector pYT3 with *ccrA* and *ccrB*; Tc^r	14
pMGPI	*S. aureus* integrative vector including the IPTG-inducible P_{spac} promoter and *lacI* gene; Ap^r Em^r	25
pSK5632	*E. coli-S. aureus* shuttle vector containing the *lac* promoter; Ap^r Cm^r	8
pMGPA	pMGPI vector with *pbpA* ribosome-binding site and the first 277 codons fused to the P_{spac} promoter; Ap^r Em^r	This study
pSKP1	pSK5632 vector with *pbpA* complete coding sequence; Ap^r Cm^r	This study

[a] Abbreviations: Mc^s, methicillin susceptible; Mc^r, methicillin resistant; Em^s, erythromycin susceptible; Tc^s, tetracycline susceptible; Em^r, erythromycin resistant; Cm^r, chloramphenicol resistant; Ap^r, ampicillin resistant.

into RN4220 by electroporation as previously described (15). The correct insertion of pMGPA into the chromosome of RN4220 via a single reciprocal crossover (a Campbell-type recombination event) was confirmed by PCR and Southern blotting. The inserted plasmid was then transferred to COL-S or COL by transduction using phage 80α as described (23), generating COL-S*spac*P1 and COL*spac*P1, respectively.

Growth of *pbpA* conditional mutants and depletion of PBP1. Overnight cultures were diluted to an OD_{620} of 0.05 in fresh TSB with IPTG (500 μM) and incubated at 37°C in an orbital shaker at 180 rpm for four generations. This "refreshment" step allowed the cells to leave stationary phase. Cultures were then washed with fresh TSB to remove IPTG and diluted to an OD_{620} of 0.05 in medium without IPTG and with different inducer concentrations (35, 50, 80, and 500 μM).

To deplete the conditional mutants of PBP1, an extra incubation step was introduced into the procedure. After the initial "refreshment" growth step, the cultures were diluted to an OD_{620} of 0.05 in medium without IPTG, incubated at 37°C in an orbital shaker at 180 rpm, and monitored carefully by OD_{620} measurements. Just before a complete halt in the increase of the OD, the bacteria were rediluted to an OD_{620} of 0.05 in fresh growth media containing different concentrations of IPTG, and their rates of growth were monitored.

Complementation assay. A 2.9-kb fragment that included the complete *pbpA* coding sequence and 300 bp upstream of it was amplified from COL DNA by PCR using primers pbp1FPstI (5′-GTATACTGCAGCAACAACCAC-3′ [PstI site underlined]) and pbp1RBamHI (5′-CAGGGATCCTCTTCTTAATCCAGAC-3′ [BamHI site underlined]). The amplified *pbpA* fragment and plasmid pSK5632 (8) were digested with PstI and BamHI and ligated, generating pSKP1. The replicative plasmid pSKP1 was introduced into RN4220 by electroporation and subsequently transferred to COL*spac*P1 by transduction, generating COL*spac*P1pSKP1.

Analysis of *pbpA* transcription by real-time RT-PCR. COL and COL*spac*P1 were grown in TSB and/or TSB supplemented with 35, 50, 80, and 500 μM IPTG. Samples were collected at an OD_{620} of 0.8 (corresponding to the OD at which COL*spac*P1 grown without IPTG stopped growing), and total RNA was isolated as described previously (31). An on-column DNase digestion using RNase-free DNase (QIAGEN, Valencia, CA) was performed to remove residual DNA. RNA was isolated from three independent cultures. The transcription levels of *pbpA* were determined by two-step real-time reverse transcriptase PCR (RT-PCR) using the relative standard curve method (user bulletin no. 2; Applied Biosystems Inc.). cDNA was generated by RT with 1 μg of DNase I-treated total RNA and TaqMan reverse transcription reagents with random hexamers (Applied Biosystems) in a total volume of 100 μl. The reaction mixture was incubated at 25°C for 10 min, 48°C for 30 min, and 95°C for 5 min. Real-time PCR was carried out with an ABI Prism 7900 sequence detection system (Perkin-Elmer Applied Biosystems). PCRs were performed, and mixtures included 1× iTaq SYBR green Supermix with ROX (Bio-Rad), 200 nM (each) forward and reverse primers, 5 μl of 1:5 dilutions of cDNA, and water to a final volume of 25 μl. Primers were as follows: PBP1forwardRT (5′-TTTTAGCATACAGTCAGCGACCA-3′) and PBP1reverseRT (5′-TCCAGGCTCGTATGTGTTTTGA-3′) were used for *pbpA* amplification, and primers ptaForRT (5′-AGAAGCAATCATTGATGGCGA-3′) and ptaRevRT (5′-ACCTGGCGCTTTTTTCTCAG) were used for *pta* amplification. The following conditions were used: 95°C for 10 min and 40 cycles of 95°C for 15 s and 60°C for 1 min. Each PCR plate contained two replicates of each sample cDNA and standard curves for each gene. These standard curves were made with six serial twofold dilutions of COL chromosomal DNA (from 2.5 ng to 78.1 pg). The specificity of the amplified products was verified by analysis of the dissociation curves generated by the ABI 7900 software based on the specific melting temperature for each amplicon. The melting curves of the PCR products were obtained by stepwise increases in the temperature from 60°C to 90°C. For all experiments, the amount of target (*pbpA*) and endogenous control (housekeeping gene *pta*) was determined from the respective standard curve by conversion of the mean threshold cycle values. Normalization was then obtained by dividing the quantity of *pbpA* by the quantity of *pta.* The normalized values of *pbpA* of COL*spac*P1 grown with the different IPTG concentrations were then divided by the normalized value of *pbpA* in COL and expressed as an *n*-fold difference relative to COL.

Electron microscopy. Strain COL was grown in TSB, and COL*spac*P1 was grown in TSB or TSB with 500 μM IPTG. When COL*spac*P1 grown in the absence of IPTG stopped growing (as indicated by no increase in the OD_{620} determined at three consecutive 10-min intervals), samples for electron microscopy were collected, centrifuged, fixed with 2.5% glutaraldehyde in 0.1 M cacodylate buffer (pH 7.0), and processed for electron microscopy according to the procedure of Ryter et al. (30), as modified by Tomasz et al. (32).

Fluorescence microscopy. COL*spac*P1 was grown in TSB or TSB with 500 μM IPTG. Samples were collected at an OD_{620} of 0.8, corresponding to the OD at which COL*spac*P1 grown without IPTG stopped growing. Cell membranes of live cells were stained with Nile red (Molecular Probes Inc., Eugene, OR) at a final concentration of 8 μg/ml for 5 min at room temperature without agitation. Fluorescence microscopy was performed with a Leica DMRA2 microscope coupled to a CoolSNAP HQ Photometrics camera (Roper Scientific, Tucson, AZ).

Immunofluorescence microscopy. Strain LH607 was grown to an OD_{620} of 0.7, and a sample was harvested and prepared for immunofluorescence essentially as described previously (26). Briefly, cells were fixed with the fixative Histochoice (Amresco) and lysed for 1 min on a polylysine-treated slide with lysostaphin (Sigma) at a final concentration of 10 μg/ml. Immunolabeling was performed

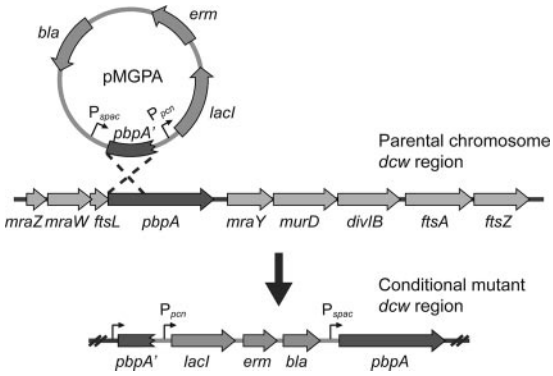

FIG. 1. Construction of the *pbpA* conditional mutant. An 850-bp fragment of *pbpA* containing the ribosome-binding site was cloned downstream of the P_{spac} promoter in the integrative vector pMGPI. The resulting plasmid, pMGPA, was introduced into *S. aureus* RN4220 by electroporation and was integrated into the chromosome by a Campbell-type recombination event. The only complete copy of *pbpA* in the resulting strain is under P_{spac} control. The fusion was subsequently moved to the COL and COL-S strains by transduction to yield COL*spac*P1 and COL-S*spac*P1, respectively.

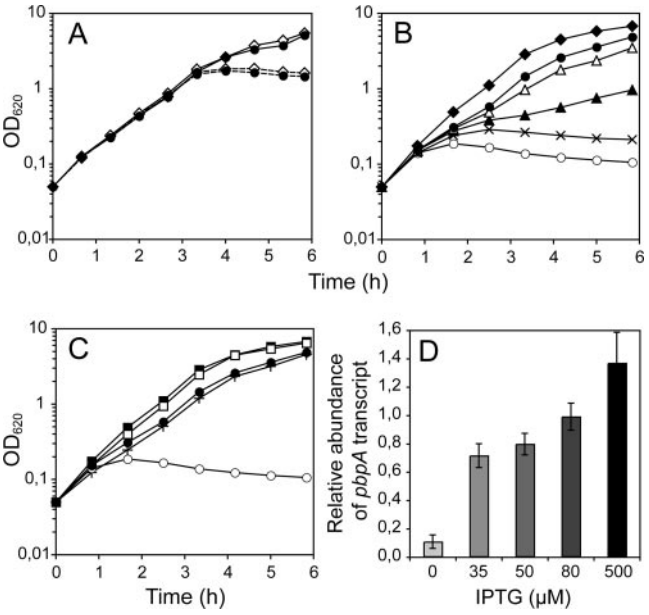

FIG. 2. Essentiality of *pbpA* expression for *S. aureus* growth and transcription of *pbpA* in the mutant strain COL*spac*P1 grown with different inducer concentrations. (A) Representative growth curves of *pbpA* conditional mutants COL-S*spac*P1 (◇) and COL*spac*P1 (●) in the absence (dashed line) and presence (solid line) of 500 μM IPTG. (B) Representative growth curves of the parental MRSA strain COL (◆) and its mutant COL*spac*P1. The mutant was depleted of PBP1 and grown in the absence of IPTG (○) and in the presence of 35 μM (×), 50 μM (▲), 80 μM (△), and 500 μM (●) concentrations of inducer. (C) Representative growth curves of COL (■), COL with pSK5632 (□), COL*spac*P1 in the absence of IPTG (○) and in the presence of a 500 μM concentration of inducer (●), and COL*spac*P1 with pSKP1 in the absence of inducer (+). (D) COL*spac*P1 was grown in increasing concentrations of inducer (see panel B), and the relative abundance of the *pbpA* transcript was expressed as an *n*-fold difference relative to COL. The transcription levels of *pbpA* were normalized to the levels of the housekeeping gene *pta*.

overnight at 4°C with anti-PBP1 antiserum diluted 1:800 in 2% bovine serum albumin in 1× phosphate-buffered saline. Cells were washed and incubated for 1 to 2 h at room temperature with anti-rabbit immunoglobulin G-fluorescein isothiocyanate conjugate (Sigma) diluted 1:500 in 2% bovine serum albumin in 1× phosphate-buffered saline. Cells were again washed, and Vectashield mounting medium (Vector Laboratories) was added. Cells were visualized by phase-contrast and fluorescence microscopy in a Leica DMRA2 microscope coupled to a CoolSNAP HQ Photometrics camera.

Peptidoglycan composition. A COL culture and a COL*spac*P1 culture previously depleted of PBP1 were used to inoculate 500 ml of TSB (COL) and TSB supplemented with 50 μM and 500 μM IPTG (COL*spac*P1). Cultures were rediluted to an OD_{620} of 0.025 and grown to an OD_{620} of 0.3 and were harvested for the preparation of cell walls. Cell walls were isolated, peptidoglycan purified, and digested with muramidase, and the muropeptide composition was determined by reversed-phase high-performance liquid chromatography (HPLC), as previously described (3).

RESULTS AND DISCUSSION

PBP1 is essential for growth of both MSSA and MRSA. Previous, unsuccessful attempts to disrupt *pbpA* in the methicillin-susceptible *S. aureus* (MSSA) strain RN4220 indicated the essentiality of this gene in MSSA (33). In order to confirm this observation and to test the essentiality of PBP1 in MRSA, a conditional mutant of *pbpA* was constructed by placing the gene under the control of the IPTG-inducible P_{spac} promoter (12). The integrative plasmid pMGPA, containing the ribosome-binding site and the first 277 codons of *pbpA*, was introduced into the MSSA strain RN4220 by electroporation, creating a strain bearing a single functional copy of *pbpA* under the control of the P_{spac} promoter (Fig. 1). The P_{spac}-*pbpA* chromosomal fusion was next transferred by transduction to the background of strain COL, an MRSA strain, and its isogenic MSSA derivative, COL-S, from which SCC*mec* had been removed by precise excision (14), generating the isogenic strains COL*spac*P1 and COL-S*spac*P1, respectively.

Neither of these conditional mutants were able to grow in the absence of IPTG (Fig. 2A), and once the strains had been depleted of PBP1, their growth rates were proportional to the concentration of IPTG in the medium, as shown for COL *spac*P1 in Fig. 2B.

The *pbpA* gene is located in a division and cell wall (*dcw*) synthesis cluster together with a number of other essential determinants, including, downstream of it, the *mraY*, *divIB*, *ftsA*, and *ftsZ* genes (28). For this reason, it was important to test whether the growth defect of the conditional mutants was due to a polar effect. The replicative plasmid pSKP1, containing the complete coding sequence of *pbpA*, was introduced into COL*spac*P1, and the strain was grown in the absence of IPTG. Growth of COL*spac*P1 in IPTG-free medium was successfully reestablished when *pbpA* was present in a plasmid (Fig. 2C).

The abundance of the *pbpA* transcripts in COL*spac*P1 grown with different IPTG concentrations was also analyzed by real-time RT-PCR. For each sample, *pbpA* values were normalized to the values of the housekeeping gene *pta*, used as the endogenous control, and expressed as an *n*-fold difference relative to COL. The successful induction of *pbpA* transcription was confirmed, and the amount of *pbpA* transcript was found to vary according to the inducer concentration present in the medium (Fig. 2D). The mutant grown with the optimal IPTG concentration (500 μM) showed an increase of approximately 1.4 times the level of *pbpA* transcript in the parental strain, COL.

TABLE 2. Inhibition of cell division and abnormal morphology in COL*spac*P1 cells grown without IPTG

Strain (growth condition)	Initial		Final		Cell diam (μm)[a]	Total no. of cells measured
	OD_{620}	CFU/ml	OD_{620}	CFU/ml		
COL*spac*P1 (without IPTG)	0.05	1.1×10^6	0.8	2.7×10^6	1.29 ± 0.02	106
COL*spac*P1 (with 500 μM IPTG)	0.05	1.2×10^6	0.8	1.7×10^7	0.89 ± 0.01	165
COL					0.88 ± 0.01	141

[a] The longitudinal length (from pole to pole) of every cell within the electron microscopy field was measured. The diameters of COL*spac*P1 cells grown without IPTG were determined only for cells belonging to major subpopulation 2, which maintain the parental ratio between the equatorial and longitudinal axes of the cells (see the text for details).

Deficit in growth rate in the *pbpA* conditional mutant. The complementation experiments clearly show that the dependence of growth of the conditional *pbpA* mutants on the IPTG inducer is related to the production of PBP1. By increasing the concentration of IPTG in the medium, it was possible to increase the growth rate of the *pbpA* conditional mutants. Nevertheless, we were never able to fully restore the growth rate of the parental strain in the conditional mutants even by supplying the highest concentrations of the inducer. The reasons for this are not clear. The possibility of insufficient expression of *pbpA* from the P_{spac} promoter was disproved by the analysis of *pbpA* transcription, which actually showed an increase in the level of *pbpA* transcript in COL*spac*P1 grown with optimal IPTG concentration. In *E. coli* and *B. subtilis*, many of the genes in the *dcw* cluster are cotranscribed in the form of long polycistronic messages, and this coordinate expression is important for normal growth (9, 10, 13, 18, 29). In the case of the *S. aureus* conditional mutants described here, *pbpA* is expressed from its native locus but not under the control of its native promoter. Furthermore, even though we have shown that the growth defect in COL*spac*P1 was unlikely to be caused by a polar effect, the *dcw* cluster is interrupted by integration of the P_{spac}-*pbpA*-bearing construct (Fig. 1). The inability to fully restore normal growth to the conditional mutant may be interpreted in the context of the genomic channeling hypothesis, according to which the clustering of *dcw* genes would favor the cotranslational assembly and function of cell division and peptidoglycan precursor synthesis complexes (19).

Changes in cell morphology during residual growth of COL *spac*P1 in IPTG-free medium. COL*spac*P1 was grown without IPTG, and the OD, viable titer, and morphology of the bacteria were tested. A parallel culture supplemented with the optimal concentration of IPTG was used as a control. After resuspension in IPTG-free medium, COL*spac*P1 continued to increase in OD, from an initial OD_{620} of 0.05 to 0.8 (Table 2). However, the initial viable titer showed only a minor increase, completely disproportionate with the 16-fold increase in OD. In the control culture, the increase in viable titer showed a precise parallel with the increase in OD.

We used transmission electron microscopy to examine the morphology of cells in populations of strain COL and the *pbpA* conditional mutant COL*spac*P1 grown in the absence or presence of IPTG in the medium. The morphological differences between these bacteria were quite striking. The parental COL cells formed a homogeneous population of bacteria, with an average ratio of 1.18 ± 0.01 between the equatorial (septal) and longitudinal axes of the cells (Fig. 3A, B, and E). In contrast, three subpopulations with distinct morphologies could be identified among cells of COL*spac*P1 grown in the absence of inducer. The first of these, subpopulation 1, representing approximately 22% of the cells evaluated, maintained both the average axis ratio and overall dimensions found in the parental COL population (Fig. 3C and F). The second and most abundant, subpopulation 2 (63% of the cells), also maintained the parental axis ratio but showed an increase of about 45% in cell size (Fig. 3C, D, and F and Table 2). The third, subpopulation 3, representing about 15% of the cells, showed an altered average axis ratio (1.7 ± 0.08), with an increased longitudinal axis (Fig. 3C and F).

Evaluation of the morphology of the COL*spac*P1 mutant grown in the presence of the optimal inducer concentration presented a picture similar to that of strain COL: cells showed homogeneous morphology, and subpopulations 2 and 3 were absent (Fig. 3E).

The existence of the distinct subpopulations when COL *spac*P1 was grown in the absence of inducer was confirmed by fluorescence microscopy using the dye Nile red to stain membranes of live cells (Fig. 3G), and quantitative evaluations of the morphologies by this method (data not shown) gave results identical to those illustrated in Fig. 3F.

We do not presently know whether the aberrant morphologies observed in bacteria "growing" with inhibited *pbpA* transcription correspond to cells with different degrees of the deleterious effects caused by depletion of PBP1 or whether they reflect the heterogeneity of the population and represent cells that were at different stages of the cell cycle when cell division was blocked by the lack of PBP1.

PBP1 and the formation of septa. Both COL and COL *spac*P1 grown without IPTG showed the same proportion of cells with signs of septation (around 80%). However, cells with complete septa represented around 90% of the COL population (Fig. 3A and H), while cells with complete septa were present in only about 15% of the COL*spac*P1 mutant population grown without IPTG (Fig. 3C and H). Interestingly, we note that depletion of *pbpA* does not seem to perturb division site selection, as most cells in the mutant population show correct placement (at midcell) of the septum even though cells with completely formed septa were rarely observed in cultures of COL*spac*P1 in the absence of inducer (Fig. 3). Moreover, the rare COL*spac*P1 cells with complete septa showed thickened equatorial cell walls. The incomplete septa may have been initiated when PBP1 was still available but were not completed due to the depletion of PBP1. Another possibility that we cannot presently exclude is that PBP1 may function only at a late stage in septum formation.

In any event, the inhibition of cell division eventually leads

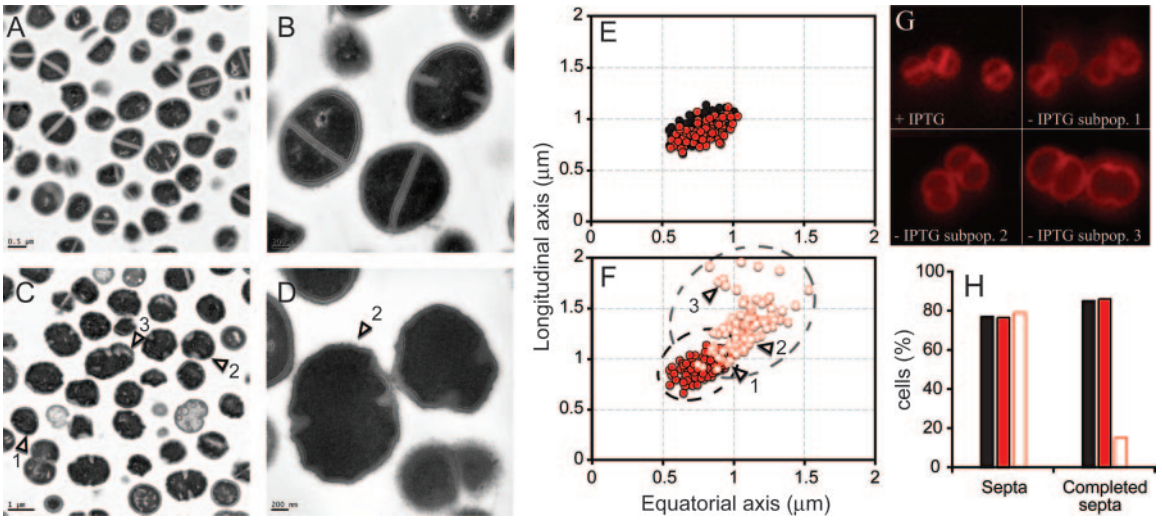

FIG. 3. Morphology of the parental strain COL and its *pbpA* conditional mutant, COL-*spac*P1, grown in the absence of IPTG. Strain COL was grown in TSB, and COL*spac*P1was grown either in TSB or in TSB supplemented with 500 μM IPTG. Thin sections were processed for transmission electron microscopy to document differences in the size and morphology of the parental strain, COL (A and B), and the mutant, COL*spac*P1, grown in the absence of IPTG (C and D). Specimens labeled 1, 2, and 3 (in panels C and D) are representative of subpopulations 1, 2, and 3, respectively, of COL*spac*P1 grown in the absence of inducer (see panel F and the text for details). (E and F) Ratio between the axes defined by the equatorial (septal) and the longitudinal planes of cells of COL (black circles) and COL*spac*P1 grown in the absence of inducer (empty red circles) or in the presence of 500 μM IPTG (filled red circles). For the purpose of this analysis, both the longitudinal and the equatorial lengths were measured from every cell within the electron microscopy field. (G) Fluorescence images of membrane-stained representative specimens of COL*spac*P1 grown in the presence of IPTG and of the three subpopulations that appear when the mutant is grown in the absence of inducer. (H) Percentages of cells that show septa (completed and/or incomplete, located at the normal equatorial position) or completed septa. Black bars, strain COL; empty red bars, COL*spac*P1 cells grown in the absence of IPTG; filled red bars, COL*spac*P1 cells grown in the presence of 500 μM IPTG.

to cells with increased size, which appear to be enveloped by a cell wall of normal thickness. The source of this cell wall material is not clear; it may result from cell wall synthesis that continues in the absence of PBP1 or may involve the redistribution of cell wall from the incomplete septa produced when PBP1 was still available.

Localization of PBP1. The striking changes in cell division detected in the *pbpA* conditional mutant raised the question of whether PBP1 localized to division sites in *S. aureus*. We therefore examined the subcellular localization of PBP1 by immunofluorescence using a rabbit anti-PBP1-raised polyclonal antibody. To prevent unspecific binding of the antibody, the protein A mutant strain LH607 was used in these experiments. The fluorescence signal was localized in the septum (Fig. 4), as was the case for COL*spac*P1 grown with 500 μM IPTG, whereas the same mutant strain depleted of PBP1 showed only background fluorescence (data not shown).

PBP1 and the chemical composition of peptidoglycan. The results in the preceding sections have shown that PBP1 is essential for growth and division. As cell wall synthesis in *S. aureus* is believed to occur mainly in the septum (26), where PBP1 is localized, we wanted to examine the composition of the peptidoglycan in the conditional mutant. For this purpose, COL*spac*P1 was grown with a suboptimal (50 μM) or optimal (500 μM) IPTG concentration, and the peptidoglycan composition was analyzed by reversed-phase HPLC. The growth rate of the culture grown at the suboptimal IPTG concentration was drastically reduced (see Fig. 2B), and yet the same conditions caused only minor alterations in peptidoglycan composition compared to the composition of the parental strain COL,

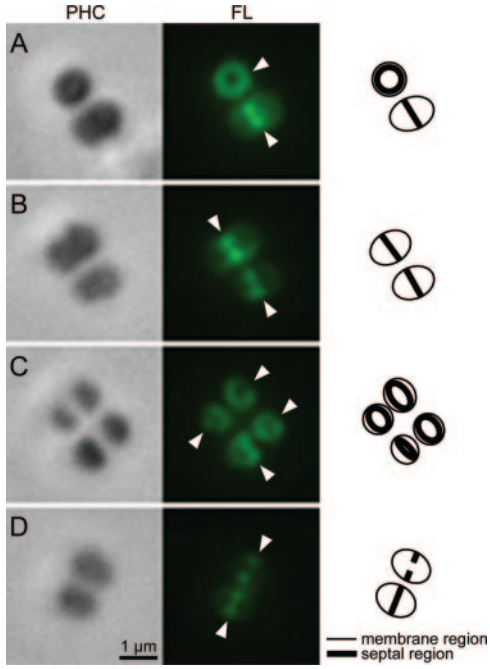

FIG. 4. PBP1 localization by immunofluorescence. Panels show selected specimens from the same field. White arrows indicate the localization of the florescence signal in septa. Phase contrast (PHC) images are shown in the first column, and florescence (FL) images are shown in the second column, followed by a schematic representation of the cells shown in each panel.

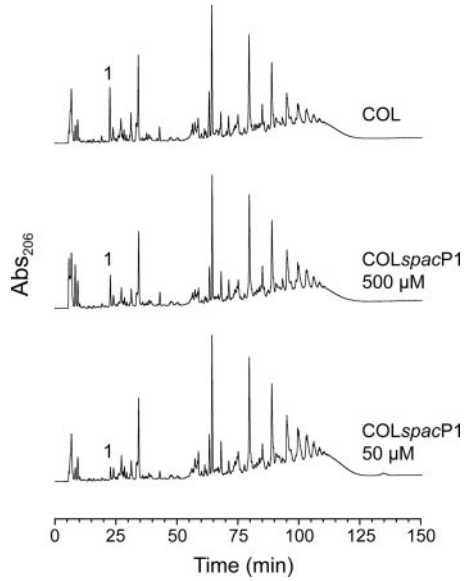

FIG. 5. Peptidoglycan HPLC profiles for strains COL and COL *spac*P1 grown with optimal (500 μM) and suboptimal (50 μM) IPTG concentrations. The deficit of PBP1 did not have a significant impact on peptidoglycan composition. The only alteration observed in the HPLC profile of the mutant grown with the suboptimal IPTG concentration was a decrease in peak 1 (identified in the chromatogram), corresponding to the unsubstituted disaccharide pentapeptide monomer.

namely, a decrease in the proportion of peak 1, representing the unsubstituted disaccharide pentapeptide monomer (Fig. 5). However, this appears to be a nonspecific alteration often observed in other mutants in the background of strain COL, some in genes not directly involved with cell wall synthesis (4; also our unpublished results). Thus, reduction in the level of *pbpA* expression sufficient to cause a significant decrease in growth rate did not cause detectable alteration in the composition of the peptidoglycan of the conditional mutant. This is in sharp contrast to the profound changes in peptidoglycan composition and cross-linking that have been described for mutants of the *S. aureus pbpD* or *pbpB* gene (16, 25).

Although we cannot exclude the possibility that alterations in the composition of the peptidoglycan in the *pbpA* conditional mutant do occur but were not detected by the particular analytical technique used, our observations suggest that PBP1 does not play a major role in the cross-linking of *S. aureus* peptidoglycan. This is also consistent with the surprising finding reported in this communication that, in contrast to the case of PBP2, PBP1 remains essential even in the background of the MRSA strain COL, which carries a constitutively expressed PBP2A. PBP2 is the only bifunctional class A HMW PBP in *S. aureus* (7, 21), and its transpeptidase activity is essential for growth in MSSA but can be replaced by PBP2A in MRSA, where its transglycosylase activity is required for optimal expression of resistance but not for growth (24, 25). The fact that PBP1, a monofunctional class B HMW PBP, carrying only the transpeptidase motifs (33), is essential for growth in both MSSA and MRSA implies that its essential function cannot be replaced by PBP2A, suggesting that its primary function may not be that of a transpeptidase.

The observations described in this communication show that the main phenotypic consequences of PBP1 depletion in *S. aureus* occur at the level of septum formation. This finding, together with the localization of PBP1 in the septum, strongly suggests that the essential role of PBP1 in *S. aureus* is linked to some specific function of this protein in cell division. The nature of this function is currently under investigation.

ACKNOWLEDGMENTS

We thank Rita Sobral and Ana Madalena Ludovice for helpful discussions and H. Komatsuzawa and M. Sugai for the generous gift of PBP1 antibody. We also thank R. A. Skurray for kindly providing plasmid pSK5632 and T. Ito and K. Hiramatsu for plasmid pSR. Real-time PCR and electron microscopy were performed at the Genomic Resource Center and at the Bio-Imaging Resource Center of The Rockefeller University.

Partial support for this study was provided by a grant (2 RO1 A1045738-06) from the National Institute of Health, U.S. Public Health Service, to A.T. and by contracts from Fundação para a Ciência e a Tecnologia, Portugal: POCTI/BIA-MIC/58416/2004 to H.L. and POCI/BIA-BCM/56493/2004 to M.G.P. S.F.F.P. was supported by grant SFRH/BD/9185/2002 from Fundação para a Ciência e Tecnologia.

REFERENCES

1. **Berger-Bachi, B., A. Strassle, and F. H. Kayser.** 1986. Characterization of an isogenic set of methicillin-resistant and susceptible mutants of *Staphylococcus aureus*. Eur. J. Clin. Microbiol. **5:**697–701.
2. **Daniel, R. A., E. J. Harry, and J. Errington.** 2000. Role of penicillin-binding protein PBP 2B in assembly and functioning of the division machinery of *Bacillus subtilis*. Mol. Microbiol. **35:**299–311.
3. **de Jonge, B. L., Y. S. Chang, D. Gage, and A. Tomasz.** 1992. Peptidoglycan composition of a highly methicillin-resistant *Staphylococcus aureus* strain. The role of penicillin binding protein 2A. J. Biol. Chem. **267:**11248–11254.
4. **de Lencastre, H., S. W. Wu, M. G. Pinho, A. M. Ludovice, S. Filipe, S. Gardete, R. Sobral, S. Gill, M. Chung, and A. Tomasz.** 1999. Antibiotic resistance as a stress response: complete sequencing of a large number of chromosomal loci in *Staphylococcus aureus* strain COL that impact on the expression of resistance to methicillin. Microb. Drug Resist. **5:**163–175.
5. **Georgopapadakou, N. H., and F. Y. Liu.** 1980. Penicillin-binding proteins in bacteria. Antimicrob. Agents Chemother. **18:**148–157.
6. **Ghuysen, J. M.** 1991. Serine beta-lactamases and penicillin-binding proteins. Annu. Rev. Microbiol. **45:**37–67.
7. **Goffin, C., and J. M. Ghuysen.** 1998. Multimodular penicillin-binding proteins: an enigmatic family of orthologs and paralogs. Microbiol. Mol. Biol. Rev. **62:**1079–1093.
8. **Grkovic, S., M. H. Brown, K. M. Hardie, N. Firth, and R. A. Skurray.** 2003. Stable low-copy-number *Staphylococcus aureus* shuttle vectors. Microbiology **149:**785–794.
9. **Hara, H., S. Yasuda, K. Horiuchi, and J. T. Park.** 1997. A promoter for the first nine genes of the *Escherichia coli mra* cluster of cell division and cell envelope biosynthesis genes, including *ftsI* and *ftsW*. J. Bacteriol. **179:**5802–5811.
10. **Harry, E. J., S. L. Rowland, M. S. Malo, and R. G. Wake.** 1994. Expression of *divIB* of *Bacillus subtilis* during vegetative growth. J. Bacteriol. **176:**1172–1179.
11. **Hartman, B. J., and A. Tomasz.** 1984. Low-affinity penicillin-binding protein associated with beta-lactam resistance in *Staphylococcus aureus*. J. Bacteriol. **158:**513–516.
12. **Henner, D. J.** 1990. Inducible expression of regulatory genes in *Bacillus subtilis*. Methods Enzymol. **185:**223–228.
13. **Henriques, A. O., H. de Lencastre, and P. J. Piggot.** 1992. A *Bacillus subtilis* morphogene cluster that includes *spoVE* is homologous to the *mra* region of *Escherichia coli*. Biochimie **74:**735–748.
14. **Katayama, Y., T. Ito, and K. Hiramatsu.** 2000. A new class of genetic element, staphylococcus cassette chromosome *mec*, encodes methicillin resistance in *Staphylococcus aureus*. Antimicrob. Agents Chemother. **44:**1549–1555.
15. **Kraemer, G. R., and J. J. Iandolo.** 1990. High-frequency transformation of *Staphylococcus aureus* by electroporation. Curr. Microbiol. **21:**373–376.
16. **Leski, T. A., and A. Tomasz.** 2005. Role of penicillin-binding protein 2 (PBP2) in the antibiotic susceptibility and cell wall cross-linking of *Staphylococcus aureus*: evidence for the cooperative functioning of PBP2, PBP4, and PBP2A. J. Bacteriol. **187:**1815–1824.
17. **Maniatis, V., E. F. Fritsch, and J. Sambrook.** 1989. Molecular cloning: a laboratory manual, 2nd ed. Cold Spring Harbor Laboratory Press, Cold Spring Harbor, NY.

18. **Mengin-Lecreulx, D., J. Ayala, A. Bouhss, J. van Heijenoort, C. Parquet, and H. Hara.** 1998. Contribution of the P_{mra} promoter to expression of genes in the *Escherichia coli mra* cluster of cell envelope biosynthesis and cell division genes. J. Bacteriol. **180:**4406–4412.
19. **Mingorance, J., J. Tamames, and M. Vicente.** 2004. Genomic channeling in bacterial cell division. J. Mol. Recognit. **17:**481–487.
20. **Morlot, C., A. Zapun, O. Dideberg, and T. Vernet.** 2003. Growth and division of *Streptococcus pneumoniae*: localization of the high molecular weight penicillin-binding proteins during the cell cycle. Mol. Microbiol. **50:**845–855.
21. **Murakami, K., T. Fujimura, and M. Doi.** 1994. Nucleotide sequence of the structural gene for the penicillin-binding protein 2 of *Staphylococcus aureus* and the presence of a homologous gene in other staphylococci. FEMS Microbiol. Lett. **117:**131–136.
22. **Okonogi, K., Y. Noji, M. Nakao, and A. Imada.** 1995. The possible physiological roles of penicillin-binding proteins of methicillin-susceptible and methicillin-resistant *Staphylococcus aureus*. J. Infect. Chemother. **1:**50–58.
23. **Oshida, T., and A. Tomasz.** 1992. Isolation and characterization of a Tn*551*-autolysis mutant of *Staphylococcus aureus*. J. Bacteriol. **174:**4952–4959.
24. **Pinho, M. G., H. de Lencastre, and A. Tomasz.** 2001. An acquired and a native penicillin-binding protein cooperate in building the cell wall of drug-resistant staphylococci. Proc. Natl. Acad. Sci. USA **98:**10886–10891.
25. **Pinho, M. G., S. R. Filipe, H. de Lencastre, and A. Tomasz.** 2001. Complementation of the essential peptidoglycan transpeptidase function of penicillin-binding protein 2 (PBP2) by the drug resistance protein PBP2A in *Staphylococcus aureus*. J. Bacteriol. **183:**6525–6531.
26. **Pinho, M. G., and J. Errington.** 2003. Dispersed mode of *Staphylococcus aureus* cell wall synthesis in the absence of the division machinery. Mol. Microbiol. **50:**871–881.
27. **Pogliano, J., K. Pogliano, D. S. Weiss, R. Losick, and J. Beckwith.** 1997. Inactivation of FtsI inhibits constriction of the FtsZ cytokinetic ring and delays the assembly of FtsZ rings at potential division sites. Proc. Natl. Acad. Sci. USA **94:**559–564.
28. **Pucci, M. J., J. A. Thanassi, L. F. Discotto, R. E. Kessler, and T. J. Dougherty.** 1997. Identification and characterization of cell wall-cell division gene clusters in pathogenic gram-positive cocci. J. Bacteriol. **179:**5632–5635.
29. **Real, G., and A. O. Henriques.** 2006. Localization of the *Bacillus subtilis murB* gene within the *dcw* cluster is important for growth and sporulation. J. Bacteriol. **188:**1721–1732.
30. **Ryter, A., E. Kellenberger, A. Birchandersen, and O. Maaloe.** 1958. Etude au microscope electronique de plasmas contenant de l'acide desoxyribonucleique. Z. Naturforsch. B **13:**597–605.
31. **Sobral, R. G., A. M. Ludovice, S. Gardete, K. Tabei, H. de Lencastre, and A. Tomasz.** 2003. Normally functioning *murF* is essential for the optimal expression of methicillin resistance in *Staphylococcus aureus*. Microb. Drug Resist. **9:**231–241.
32. **Tomasz, A., J. D. Jamieson, and E. Ottolenghi.** 1964. The fine structure of *Diplococcus pneumoniae*. J. Cell Biol. **22:**453–467.
33. **Wada, A., and H. Watanabe.** 1998. Penicillin-binding protein 1 of *Staphylococcus aureus* is essential for growth. J. Bacteriol. **180:**2759–2765.
34. **Weiss, D. S., K. Pogliano, M. Carson, L. M. Guzman, C. Fraipont, M. Nguyen-Disteche, R. Losick, and J. Beckwith.** 1997. Localization of the *Escherichia coli* cell division protein Ftsl (PBP3) to the division site and cell pole. Mol. Microbiol. **25:**671–681.